NTNU
Norwegian University of
Science and Technology

Monte Carlo simulation to study the interaction between the weak polyelectrolytes and two oppositely charged nano particles. Influence of nano particle separation and pH variation.

Binamra Shrestha

MSc in Physics
Submission date: May 2017
Supervisor: Rita de Sousa Dias, IFY

Norwegian University of Science and Technology
Department of Physics

Preface

This is Master's thesis, in department of physics, at Norwegian University of Science and Technology as a part of the MSc Physics program. The work has been carried out at second year of the master's program in the academic year 2016/17.

The reader is expected to have the background on computational physics, colloidal chemistry, and physical chemistry.

Acknowledgement

I would like to heartily thank my supervisor, Associate Professor Rita de Sousa Dias who has supported me throughout the year in developing this thesis. It is with her generous support I have come this far along the project.

I would also like to thank Morten Stornes, PhD candidate who have helped me with every small query I had.

Abstract

Interaction between weak polyelectrolytes and two oppositely charged nano particles is studied with Monte Carlo simulation. It is seen that the nano particle separation, and pH of the solution influence the titration of the polyelectrolytes and the interaction of polyelectrolytes and nano particles. The interaction influences the conformational properties of the polyelectrolytes and the charge distribution along polyelectrolytes chain. It is seen from radial distribution function of nano particle and polyelectrolytes that weak polyelectrolytes interaction with the nano particles is stronger than the strong polyelectrolytes Attractive mean force between the like charge nano particles in presence of monovalent counterion and monovalent monomers of polyelectrolytes is observed. Attractive force is mainly from the contribution of bond force of the polyelectrolyte chain.

Abbreviations

PEs – polyelectrolytes

NPs – nano particles

g_{ij} – radial distribution function of particle i to particle j

S_{NP} – NP – NP separation

r_g – radius of gyration

RDF – radial distribution function

Pmf – potential of mean force

Contents

List of figures

1. Introduction

The study of like charged nano particles (NPs) and polyelectrolytes (PEs) has an immense importance in the colloidal chemistry. The variety of processes involving in the industrial and commercial use have NPs and PE as central of their concern.(1, 2) Understanding the virtue of forces acting upon the particles are is central in determining the phase of the system. The force between like charged particles is effectively only repulsive but it has been documented that net attractive force can be generated in system with high electrostatic coupling and multivalent counterion.(3-5) Polyelectrolytes (PEs) interacts with the NP which changes the conformation of PEs.(6-9) It is crucial to understand the nature of the interaction between them as it involved in biological systems.(10)

Polyelectrolytes can be classified as polyanions, polycations or polyampholyte depending on the type of charge it contains. Another classification is weak and strong PEs.

In strong PEs charge distribution along the PE only depends on the initial chemistry and remains uniform over the large pH variation. In the other hand the charge distribution of weak PEs is sensible to the pH variation. Hence in the case of weak polyelectrolytes, conformational changes depend on the ionic concentration, pH, PE concentrations, NP concentration, NP charge.(9, 11, 12)

In this study, we have focused on the study of the polyanion interacting with two positively charged NPs. The NPs are fixed at a separation from each other, and a fixed pH. We investigated for different pH and separation between the NPs. Compare to the real scenario NPs can be taken as globular protein while polypeptides are PEs.(13, 14) Interaction between two like charged particles were studied as charged parallel plates.(15) Linse used Monte Carlo simulation to calculate the mean force between the like charged macromolecule to show that at high electrostatic coupling net attractive force is generated.(3) A recent study done by Salerno, Frischknecht and Stevens using Density Functional Theory and molecular dynamics showed that the interaction between the NPs can be attractive with divalent and multivalent counterions.(5) In many simulation attractive force seems to be an short range character originating from correlation effect. Many studies have been done with weak PE interacting with charged nanoparticles. Stoll and co-authors have studied the

influence of stiffness on PE complexion(16), pH, charge mobility, and ionic concentration.(6) Ulrich, Seijo and Stoll studied differernt types of complexion that can be formed(7), influence of explicit ions on titration curve and conformation of PEs(17). Skepo and Lines have studied the system with a PE and multiple NPs.(18) Jonsson and Linse have studied the PE and macroion complextion in respect to linear charge density, chain length, and macroion charge.(19)

In this study, we focus to expand our knowledge on how the weak PEs can influence the mean force between the like charged NPs and study the conformation of the PEs chain.

2. Model

2.1. Primitive Model of Electrolyte

In this work, we study the interaction between a polyelectrolyte (PE) chain, and two colloids (here referred to as nano particles, NP). The system also contains the counterion for the PE and NP.

The primitive model of electrolytes is adopted throughout the system as it provides a good basis of statistical mechanical description of charged colloids.

The components of the system are represented by hard spheres, differing in charge and size. The solvent enters the solution only through its relative permittivity with permittivity constant $\epsilon_r = 78.4$ Solution containing only the charged colloids and their counterions with a PE chain and its counterion, forming electroneutral system are studied. Monte Carlo (MC) simulation are performed at temperature T =298 K in the grand canonical ensemble according to the Metropolis algorithm.

Properties of interest govern the choice of boundary condition. Normally there are three types of boundary condition spherical, cylindrical, and cubic box. For this study, cylindrical boundary condition is used.

The radius of NP R_{NP} = 20 Å, and that of NP's counterion is R_C = 2 Å.

There are two NPs fixed at z-axis at different separation between NPs (S_{NP}). The charge is fixed at 60e at the center to obtain a homogeneous charge distribution at the surface of the NP, e is the elementary charge. A total of 120 counterions, has radius of 2 Å and charge -1e.

One linear polyanion is generated. A simple hard sphere is used to eliminate the internal atomistic degree of freedom. The chain in freely jointed, succession of 60 hard beads. Along with polyanion, 60 counterions are also generated. Each monomer and the counterions have radii of 2 Å.

Each PE monomer charge is pH dependent, each monomer is a titrating site which can be neutral of negatively charged (-1e).

When a monomer of PE chain in charged a PE counterion is also charged to maintain electroneutrality.

There are theories proposed to explain the potentiometric titration of weak PEs.(11, 20-24) To understand the formulation of the titration of PE chain, let us take the case of acidic monomer. The dissociation constant K_0 of a weak acid HA can be described, according to the law of mass action as

$$K_0 = \frac{[H^+][A^-]}{[HA]} \quad (1)$$

From this equation, the pK_0, negative decadic logarithm can be calculated as

$$pK_0 = pH - \log\frac{[A^-]}{[HA]} \quad (2)$$

For a weak acid, $[A^-]$ can be related directly to the degree of ionization (α') and [HA] to (1 – α'). Finally, the pK_a value can be calculated by means of the Henderson-Hasselbalch equation (book reference)

$$pK_0 = pH - \log\frac{\alpha'}{(1-\alpha')} \quad (3)$$

In case of the acid/base PE K_0 is different for each monomer which is dependent on the ionization of the neighboring site. This is simplified by the mean field approximation, which assumes a single K_a for all the titrating sites so that

$$pK_a = pH - \log\frac{\alpha}{(1-\alpha)} \quad (4)$$

Where α is the average ionization of the PE chain. For $(\alpha \to 0)$, $pK_a = pK_0$. The difference between apparent dissociation constant and acidic monomer is

$$\Delta pK = pK_a - pK_0 = pH - pK_0 - \log\frac{\alpha}{1-\alpha} \quad (5)$$

Therefore, removing a proton from PE chains is increasingly difficult when the degree of ionization α increases leading to the increase of the apparent dissociation constant.

During the MC simulation, acceptance of each protonation/deprotonation step of the PE monomers is related to the MC metropolis election criterion as follows.

$$\Delta E = \Delta E_c \pm K_B T\, ln10(pH - pK_0) \quad (6)$$

Where k_B is the Boltzmann constant (1.3807×10^{-23} J K $^{-1}$) and T is the temperature (298 K). The second term represents the change in free energy of the intrinsic association reaction of a monomer. The signs minus and plus are used when the monomers are deprotonated and protonated, respectively. The value pH – pK_0 is used as an input parameter varying from -4 to 5.

The potential energy of the system is given by

$$U = U_{hs} + U_{elec} + U_{ext} + U_{bond} \quad (7)$$

Where

$$U_{elec} = \sum_{i<j} u_{ij}^{elec}\left(r_{ij}\right) \quad (8)$$

$$u_{ij}^{elec}(r_{ij}) = \frac{Z_i Z_j e^2}{4\pi\varepsilon_0\varepsilon_r r_{ij}} \quad (9)$$

where Z_i is the charge of particle *i*, ϵ_0 is the permittivity of the vacuum, ϵ_r is the relative permittivity of the solvent, *r* is the distance between the center of the two interacting particles.

In this model, the NPs are place at the z-axis of the cylinder, and the confining external potential, applying to all the particles is given by

$$U_{ext} = \sum_i u_i^{ext}(r_j) \tag{10}$$

$$u_i^{ext}(r_i) = \begin{cases} \infty & otherwise \\ 0 & \sqrt{(x_i^2 + y_i^2)} < R_{cyl} \; and \; |z_i| \leq {}^{L_{cyl}}/_2 \end{cases} \tag{11}$$

Where R_{cyl} denotes the radius of the cylinder and L_{cyl} denotes the length of the cylinder. S_{NP} is held fixed at the z-axis for most the calculations. To reduce the dependence of effect of the size of the cell radius of NP ($R_{NP} \ll R_{cyl}$) and separation ($S_{NP} \ll L_{cyl}$).(3)

In the previous study it has been shown that the shape of the cell has no effect on the NP interaction given that $L_{cyl}/2$ is larger than the S_{NP} and R_{cyl} is larger than the R_{NP}.

The bond force is given by

$$U_{bond} = \sum_{i=1}^{N_{bead-1}} \frac{1}{2} k_{bond}(r_{i,i+1} - r_0)^2 \tag{12}$$

Where N_{bead} is the number of monomer, $r_{i,i+1}$ is the length of bond between i and $i+1$ particle of the chain, r_0 = 5 Å is the unperturbed equilibrium distance and k_{bond} = 0.4 Nm-1 is the force constant.

In this study, the thickness of the first layer of monomer adsorption Ads around the NPs is defined as

$$R_{NP} + R_m \leq A_{ds} \leq R_{NP} + 3R_m \tag{13}$$

The PEs is considered adsorbed when center of any of the monomers lies in the A_{ds} limit. When PEs is adsorbed to both the NPs simultaneously it is considered as bridge formation.

The analysis done are degree of ionization of weak PE chain, root mean square of radius of gyration ($<r_g^2>^{1/2}$) of the PE, radial distribution function of a particles to every other particle, fraction of MC steps with bridge formation, mean force, and potential of mean force between the NPs and degree of ionization each monomer in the weak PE chain. Only two components S_{NP} and pH-pKa values are varies throughout the simulation.

The control systems are also separately studied. The different control systems are system with only one NP with its counterion, system with two NPs with its counterion, system with weak PE chains only, system with strong PE chain in presence of NPs are also simulated. In case of strong PE to make comparison with weak PE, each monomer of strong PE charge equals to degree of ionization (α) calculated at particular pH-pK_0 and separation of NPs. Strong PE is then simulated in the system with same S_{NP} and compared with the respective weak PEs.

All simulations were performed using the MOLSIM package, v. 6.0.5(25)

2.2. Mean force and potential of mean force

The mean force and the corresponding potential of mean force between the two NPs mediated by their counterions in the absences and the presence of PEs is discussed. As all the particles are confined in a cell, and all of them interact with each other, the force calculated is a summation of interaction of all the particles, rather than only two NPs, hence it is called mean force

Since the NPs and counter ion are confined in the cell, this takes in account the interaction of surrounding electrolyte, the force is mean force rather than effective force.

The mean force F operating on one of the NP, projected on the NP-NP inter particle vector R_{NP} defined as

$$F(r) \equiv \sum_{i \neq NP}^{n} \langle -\nabla_{rNPi} u_{NPi}(r_{Mi}) \rangle \tag{14}$$

with F(r) > 0 implying repulsive mean force and F(r)<0 attractive mean force. <…> denotes an ensemble average of the positions of the counterions. The related U^{pmf} is defined by

$$U^{pmf} = -\int_{\infty}^{r} F(r')dr' \tag{15}$$

Step wise numerical integration was used to calculate the potential of mean force.

At large r, F(r) and U^{pmf} approaches zero. For many systems, the mean force has not decayed to zero, the conventional $U^{pmf} = 0$ for infinite separation cannot be employed. So U^{pmf} (r = 88 Å) = 0 has been assigned.

Both quantities (mean force and potential of mean force) depend on direct NP-NP interaction and indirect contribution mediated by the PE and counterions.

From the principle of local equilibrium, the mean force can be express in different ways.(4, 26) One of them which is numerically advantageous is known as mid-plane approach.

2.2.1. Midplane approach for calculation of mean force

In this approach, the surface of integration is one half of the cylinder.

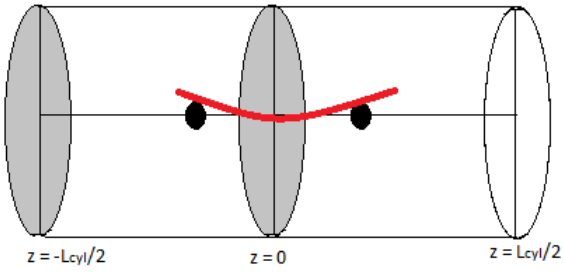

Figure 2-1 Illustrative diagram of cylindrical cell with two NPs at the sides centered at z=0 plane. The red line represents PE chain. Mean force is measured at z=0 plane.

The mean force can be divided into three terms as

$$F(r) = F_{ideal}(r) + F_{hs}(r) + F_{elec}(r) + F_{bond}(r) \quad (16)$$

$$F_{ideal}(r) = kT\left[\rho_I(z=0) - \rho_I\left(z = L_{cyl}/2\right)\right]A \quad (17)$$

$$F_{elec}(r) = \sum_{i<j}^{N}{}' < -\nabla_{r_{ij}} u_{ij}^{elec}(r_{ij}) > \quad (18)$$

$$F_{hs(r)} = kT\left[\left(\frac{\langle N_c\rangle}{|dz|}\right) - \left(\frac{\langle Nc\rangle}{(-dz)}\right)\right] \quad (19)$$

$$F_{bond}(r) = \sum_{m=1}^{N}{}' < -\nabla_{ij} u_m^{bond}(r_{ij}) > \quad (20)$$

$F_{ideal}(r)$ arises from the difference in the transfer of the linear moments of the counterions across the plane (z=0) and ($z = L_{cyl}/2$). As $r << L_{cyl}/2$, $F_{ideal}(r)$ is dominated by the $\rho_I(z=0)$ term.

$F_{elec}(r)$ is the average force operating across the plane z = 0 from the electrostatic interaction among the charged particles and the ($'$) denotes that summation only includes pairs of the particles located at the different side of the planes z = 0.

$F_{hs}(r)$ is the average force across the midplane through hard sphere contact.

F_{bond} represents force across the midplane transmitted by the harmonic bonds.

The evaluation of the densities at the z-planes in equation 17 requires a numerical method. The method used for the current study can be described as:

$$F_{ideal}(r) = kT \lim_{\Delta h \to 0^+}\left[\frac{< N_I >_{\Delta h}^{0}}{\Delta h} - \frac{< N_I >_{\Delta h/2}^{-} + < N_I >_{\Delta h/2}^{+}}{\Delta h/2}\right] \quad (21)$$

Here $<N_I>^0_{\Delta h}$ is the average number of particles in the slab Δh centered at z=0 and $<N_I>^{\pm}_{\Delta h}$ is the average number of particle in the slab $\Delta h/2$ centered at $z = \pm(L_{cyl}/2 - \Delta h/2)$. The small Δh gives

improved measurement of F_{ideal} but is subjected to large number of statistical error. Whereas large Δh reduces the statistical error but increases the systematic error.

Calculation of $F_{elec}(r)$ is straight forward. $F_{hs}(r)$ is evaluated by the virtual displacement of the segments and counterions near z=0 plane toward the plane z=0 and checking for the hard sphere overlap.

Parameter Optimization

F_{ideal} and F_{hs} are dependent on parameters Δh and dz respectively in terms of numerical calculation. Optimization of these values according to our system is necessary to get good result with statistically negligible errors.

Systems with S_{NP} = 41 Å without PEs were simulated and F_{ideal} was calculated for different ΔH. Figure shows the F_{ideal} values for S_{NP} = 1 Å. F_{ideal} should be maximum as most of the particles tend to be in between the NP at z=0 plane. This can be observed at values ΔH = *0.1 Å, 0.01 Å and 1 Å.* For ΔH = *0.1,* F_{ideal} is the highest and has the least error, compare to that of Fideal (0.01) which has comparable value but has relatively higher error and $F_{ideal}(1)$ is not considered because ΔH = *1*

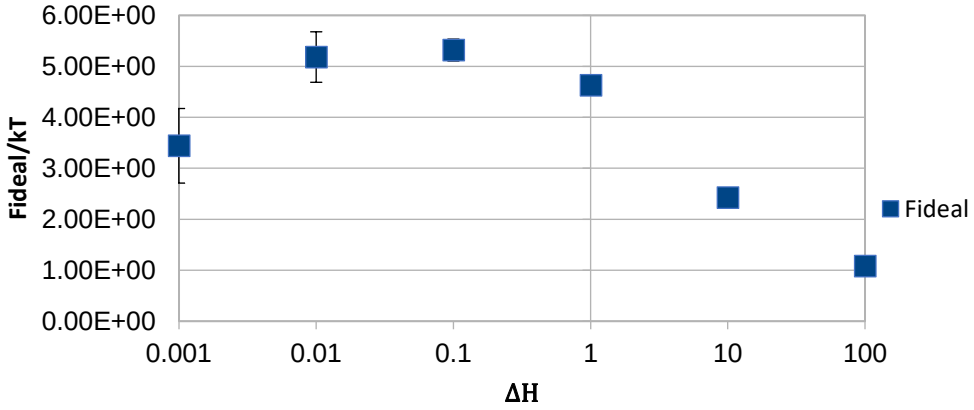

Figure 2-2 Fideal computed with different ΔH value to optimize the value.
From the figure ΔH = 0.1 is considered as the optimized value.

is the same order of radius of monomers and can cause systemic error. Therefore, ΔH = 0.1 is the optimized value and is set for the entire calculation.

Figure (2-3) shows the f_{hs} for S_{NP} = 41 Å without PEs at different values of *dz*. From the figure (), it can be observed *dz = 0.05* has the most favorable value with the least error (not observable in figure). Therefore, the value of *dz* =0.05 is set for the entire system.

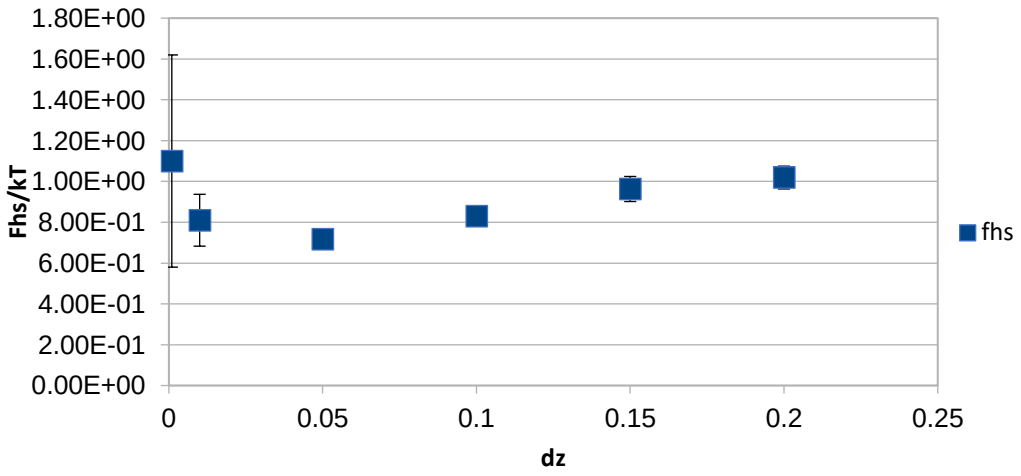

Figure 2-3 F_{hs} calculated for different dz to optimize the value of dz. From the figure dz=0.05 is considered the most optimized as it has the least error among all the values.

3. Result and Discussion

3.1. One and two NPs in solution with respective counterions

We have started by comparing the system with 1 NP and 2 NPs at the different separation in the absence of PE.

3.1.1. RDF between the NP-counterion

Representative radial distribution functions (RDFs), $g_{ij}(r)$ are shown in figure (3-1). These function displays the relative density of a particle *j* at a distance *r* from a particle of type *i*. At distances $r < R_i + R_j$, where the hard sphere overlap appears, $g_{ij}(r)$ is exactly zero. If the particle is found at $r = R_i + R_j$, then it shows the particles are in contact.

Figure (3-1) shows the RDF between the NP and counterion for the system with 1 NP, and 2 NPs with S_{NP} = 41 Å, 44Å and 92 Å. The sharp peak indicates that counterions are localized at r = 22.5 Å, which is the contact point between the NP and the counterion. The magnitude for the of the peak

for 1 NP system is nearly 3 times higher than that of system with 2 NPs. Two NPs system has higher surface area compare to that of 1 NP system. Therefore, number density of counterion is

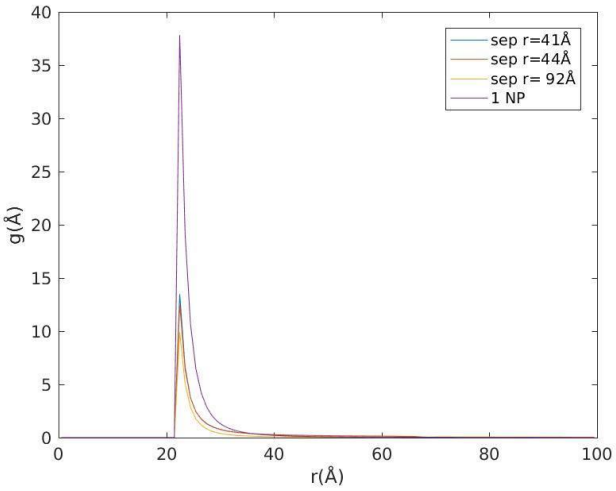

Figure 3-1 RDF of NP-counterion in 1NP system, 2 NP system S_{NP} =41 Å, 44 Å, 92 Å. The peak at r = 22 Å shows counterion localization at NP surface.

higher at the 1NP system. It also shows counterion localization at the surface of the NP.

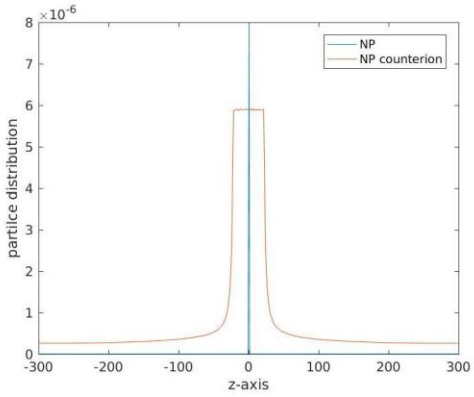

Figure 3-2 Particle distribution along z-axis. The counterion is distributed symmetrically around the NP.

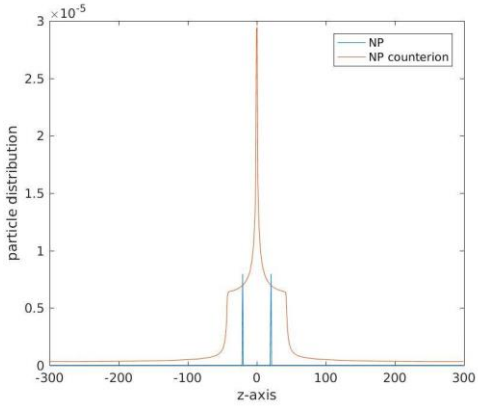

Figure 3-3 Particle distribution along z-axis with two NP system S_{NP} = 41 Å The counterions are highly concentrated at the space between the NPs.

The figure(3-3 – 3-5) shows the distribution of counterions along z-axis. For the system with 1 NP the counter ions are distributed symmetrically around the NP placed at z =0. Such is not seen for

the system with two NPs. Here the counterions are concentrated in the space between the NPs. This higher concentration of counterion in between the NPs than the other side is seen even up to the separation r = 170 Å.

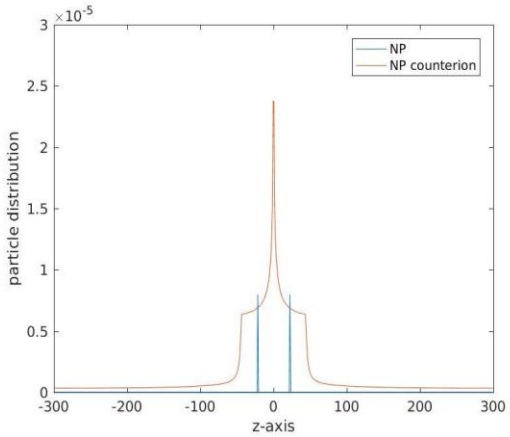

Figure 3-4 Particle distribution along z-axis with two NP system S_{NP} = 44 Å

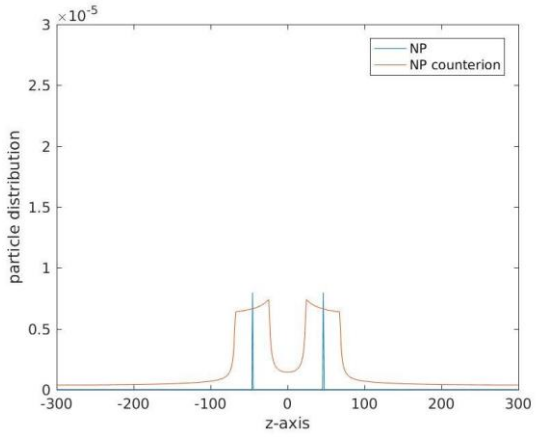

Figure 3-5 Particle distribution along z-axis with two NP system S_{NP} = 92 Å

3.1.2. RDF between counterion–counterion is discussed below.

Figure (3-1) shows (RDF) between the counterion-counterion in systems with 1 NP and two system of 2 NP with S_{NP}= 41 Å and S_{NP} = 92 Å.

In the systems with 1 NP and 2 NPs with S_{NP} = 92 Å, the distribution peaks at counterion-counterion distance r = 7.5 Å. The nature of three curves are similar but differ in the magnitude of

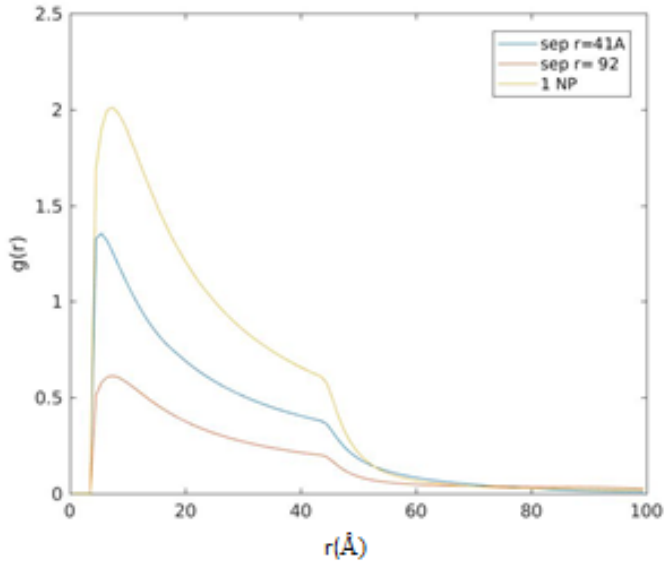

Figure 3-6 RDF of counterion-counterion in the system with 1NP, 2NP with S_{NP}= 41 Å and 92 Å. The peak for the two curve is at r = 4.5 Å for 1 NP and 2 NP at S_{NP} = 92 Å. For 2 NPs system at S_{NP} = 41 Å the peak is at 4.5 Å

the peak. Peak is highest in the system with 1 NP. Compare to the system with 2 NPs at S_{NP} = 41 Å, the peak decreases. As the surface area of 2 NPs is larger, the counterion density decreases.

In the system, S_{NP} = 41 Å the peak is at shorter separation r = 4.5 Å compare to that of r = 7.5 Å in 1 NP system. In 2 NPs system counterions concentrates in between the NPs as seen in figure (3-3) which increases the local density in that space. This cause the average distance between the counterions to decrease.

3.2. Mean Force and Potential of Mean Force.

Measurement of mean force was carried out for different separation of the NPs centered at z=0. Figure (3-7) shows mean force F(r) studied for all separation. The largest magnitude calculated for S_{NP}= 41 Å is F(S_{NP} = 41 Å) = 8 kT. It decays as separation increases.

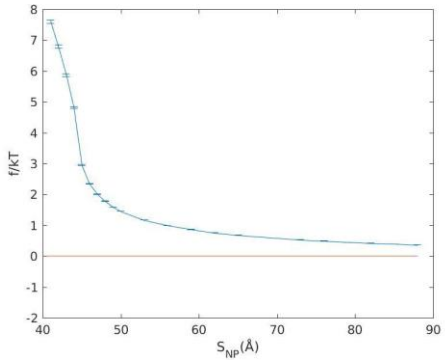

Figure 3-7 Mean force of two NPs system.

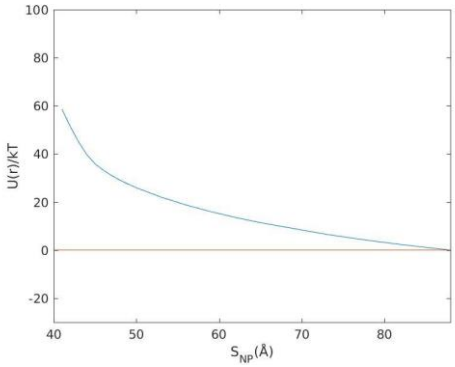

Figure 3-8 PMF of two NPs system

Figure (3-9) shows the different components of F(r). $F_{ideal}(r)$ is the highest contributor to the repulsive force. It decays as separation increases. As NP separation increases particles are less concentrated in the plane z=0 and so the ideal force decreases. $F_{elec}(r)$ is repulsive but shows a minimum at $F_{elec}(44) \cong 0$. This minimum arises from counterion correlation but since only monovalent ions are present, these are not strong enough to reduce attraction between the NPs.

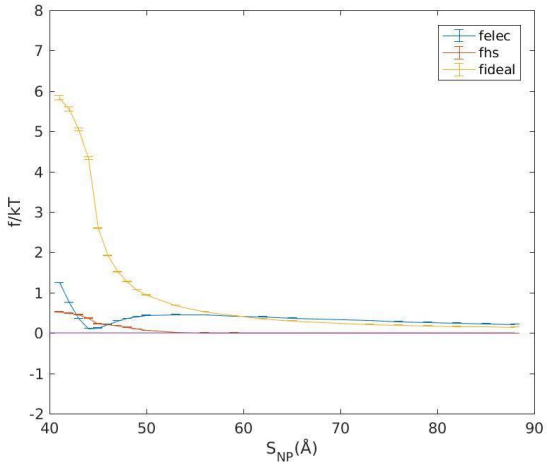

Figure 3-9 Components of mean force presented separately. F_{ideal} is the entirely repulsive. F_{elec} has a well due to counterion correlation. This is not enough to induce an attractive force.

The potential of mean force is shown in figure (3-8). For the very short separation the pmf tends to infinity and it decays smoothly towards zero for large S_{NP}.

3.3. Polyelectrolyte behavior

3.3.1. Titration Curve

As the charge in the PE chain is dependent on the pH of the solution, it is important to understand how the titration curve varies at systems.

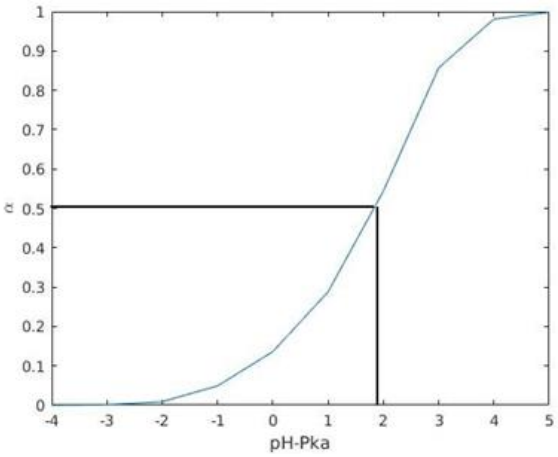

Figure 3-10 Titration curve of weak PE in absence of NP

Figure (3-10) shows the titration curve of the PE chain. The degree of ionization (α) = 0.5 for pH-pK_0 = 2

3.3.2. RDF of PE-counter ion

RDF of weak PE-counterion is given in the figure (3-11). The strong counterion condensation is observed for the systems where α > 0.5.

A comparative study is done with the strong PEs. Strong PEs with monomers having charge as α of the weak PEs are simulated.

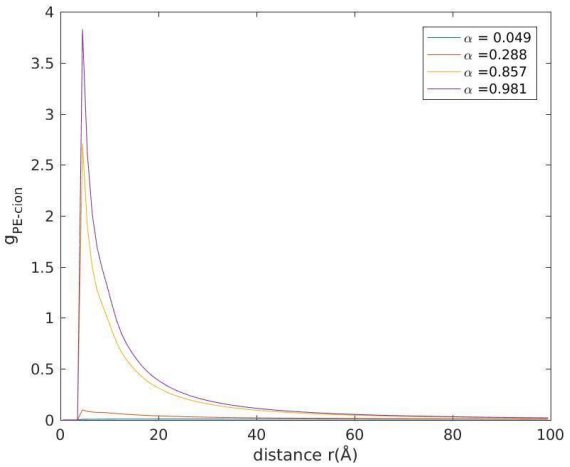

Figure 3-11 RDF of weak PE chain with its counterions

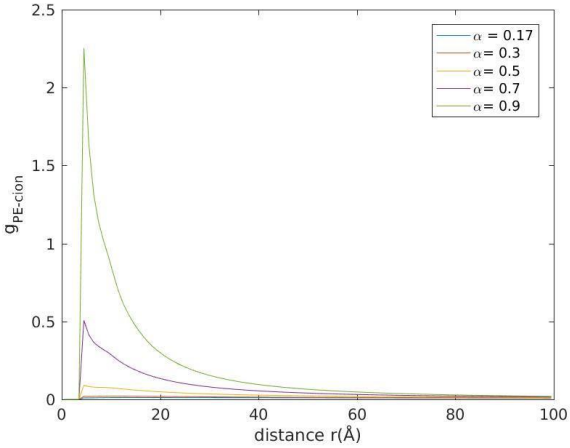

Figure 3-12 RDF of strong PE chain with its counterions

Figure(3-14) shows the RDF of strong PEs. RDF is significantly lower. For α = 0.7 maximum g_{PE-C} = 0.5 and at α = 0.9 maximum g_{PE-C} = 2.25 which is 5 and 2 times lower than the values obtained for the weak PE, respectively.

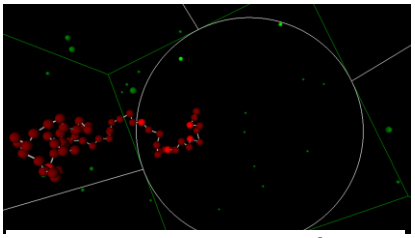

Figure 3-13 Snapshot of weak PE chain at pH-pKa = -4

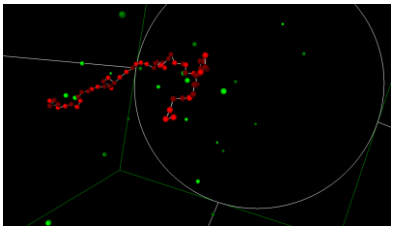

Figure 3-14 Snap shot of weak PE chain at pH-pKa = -1

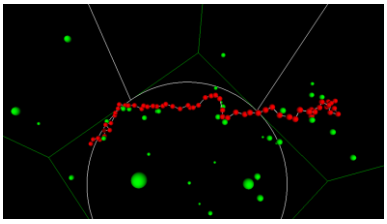

Figure 3-15 Snap shot shot of weak PE chain at pH-pKa =4

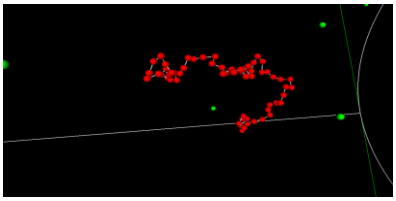

Figure 3-16 Snapshot of strong PE at α = 0.3

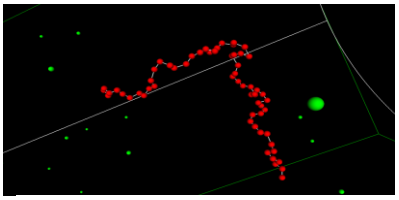

Figure 3-17Snapshot of strong PE at α = 0.5

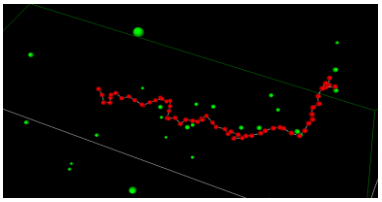

Figure 3-18 Snapshot of strong PE at α=0.9

This suggests that interaction between weak PE and counterion is stronger for weak PEs than for strong PEs, for the same charge. From equation (13) electrostatic potential between the particles is

proportional to the product of their charges. In case of strong PEs the charges of the monomers and the counterions are fractional so the interaction between them is weaker than the interaction in weak PEs where the charges are unit e.

Figure (3-13) to (3-15) shows representative snapshots of the weak polyelectrolyte as different pH-pKa values. The bright red particles are the charged monomers and the dark red particles are the uncharged particles.

Figure (3-16) to (3-18) show the snapshot of strong PE at different PE charge. At lower charge the counterions are not seen near the PE chain as they have weaker interaction.

3.3.3. Radius of Gyration

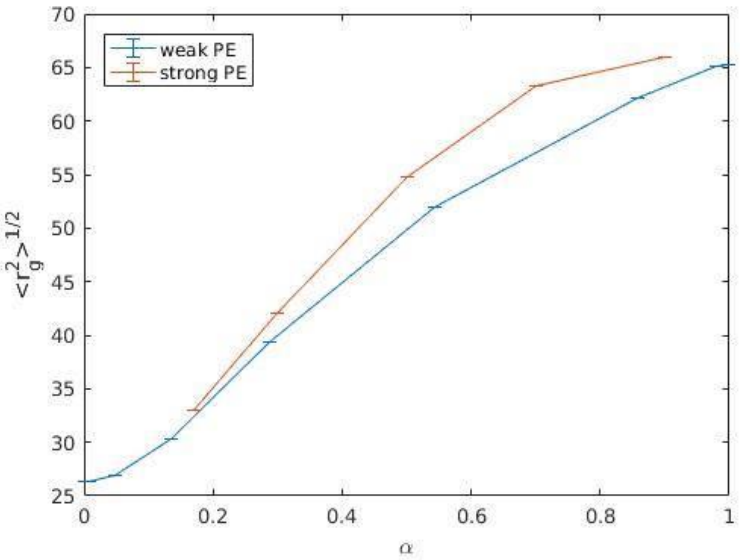

Figure 3-19 Radius of gyration of strong and weak PE at different α.

The root mean square of radius of gyration $<r_g^2>^{1/2}$ is defined as root of squared average distance between each monomer and its center of mass. The figure (3-19) shows the comparison between weak and strong PE as function of α. Rms of the radius of gyration for both PE has a linear relationship α. The repulsion of neighboring charged monomers causes the PE to expand as seen in the representative snapshots of figures (3-16). Radius of gyration of strong PE is more than that weak PE.

Counterion condensation in weak PE is significantly higher than that of strong PE. This provides screening of charged monomer and the repulsive force is minimized which reduces the radius of gyration.

3.4. Polyelectrolyte interaction with NP

3.4.1. Degree of ionization

The presence of NPs significantly influences the degree of ionization. As the monomers get adsorbed to the NP it gets easier to 'deprotonate' the monomers in the vicinity of the NP, shifting the inflection point in the titration curve to much lower pH-pK_a values when compared to free PE. The NP separation also influences the α. Shorter separations leads to higher α at lower pH-pK_a. At

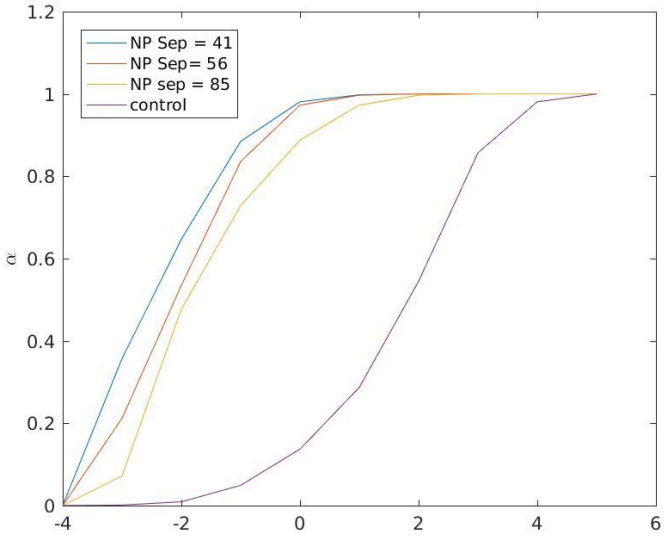

Figure 3-20 Degree of ionization of weak PE at different NP separation with respect to pH-pK_a

shorter separation r= 41 Å α reaches unity at pH-pK_a = -1, for S_{NP}= 85 Å α reaches unity at pH-pK_a = 1.

3.4.2. Radial distribution function of NP-counterion and NP-PE

The radial distribution function of NP-counterion and NP-PE give us an insight on how strongly the different component interact. The observation is divided into three regimes, with low,

intermediate and high pH-pK_a (-4, -1, 4) values, respectively. In each regime, RDF is discussed for 3 NP separations r=41 Å, 62 Å, 88 Å

RDF NP-counterion

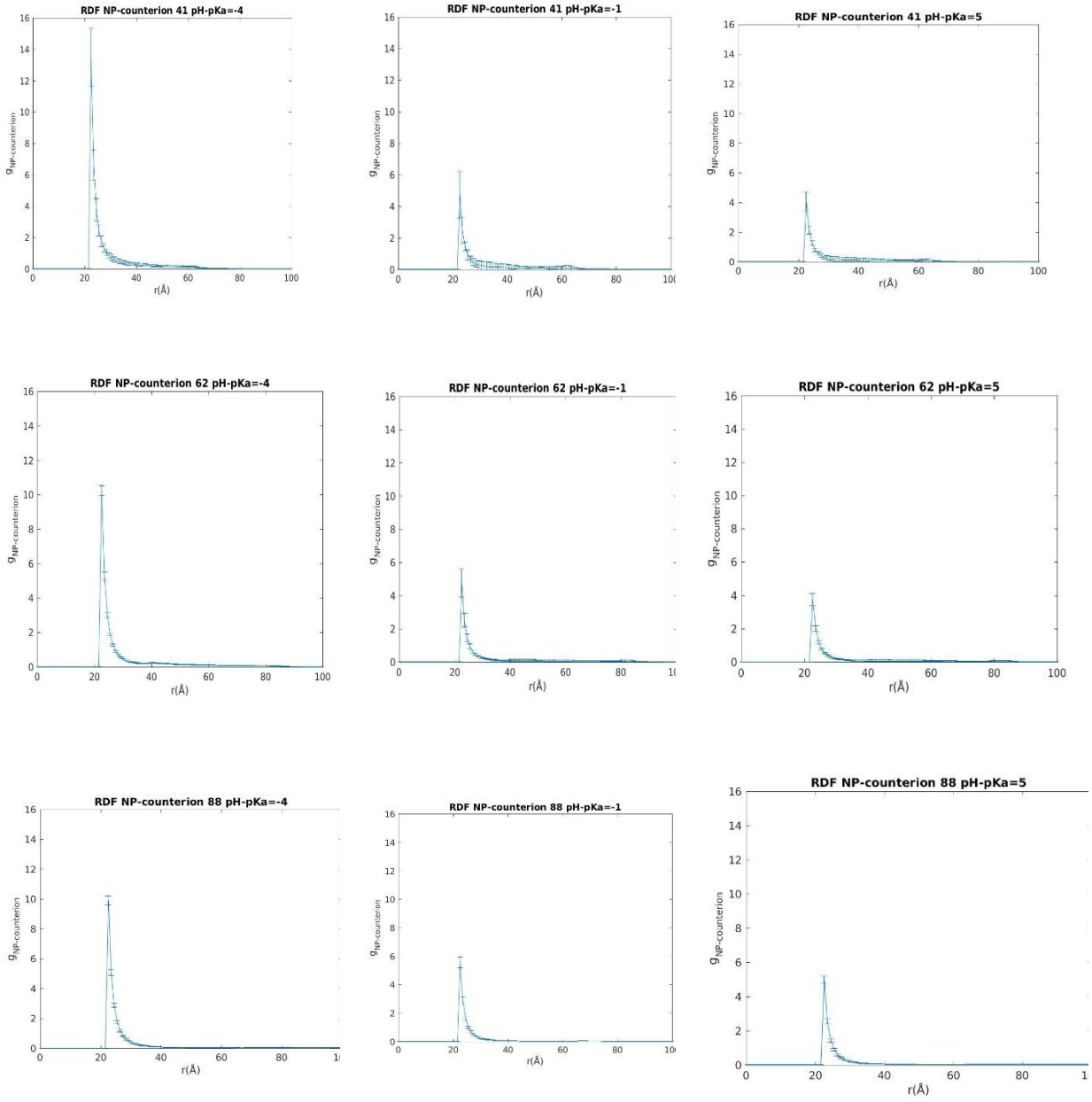

Figure 3-21 RDF of NP-counterion at different NP separation and different pH-pK_a

Figure (3-21) shows the RDF of NP-counterions for different systems as indicated as the heading of the figure. The peak in all the three regimes and three different NP separation, shows that the

counterion is localized at the NP surface. For low pH regime (top panels), the peak values correspond to the one with RDF of NP-counterion without PE (figure (3-14)). This shows that the presence of the uncharged PE does not affect the NP-counterion interaction. The peaks in the intermediate pH regime (middle panels) is half the value for that of the low pH regime. This is mainly due to the interaction PE NPs which weakens the interaction between the NP and counterion. The high pH regime (lower panel) shows a similar distribution than that of the intermediate pH regime.

RDF NP-PE

Figure (3-22) shows the RDF of the NP-PE for different systems, as indicated at the heading of the figures. The RDF of NP-PE for low pH regime (top panels) has values equal to zero representing that PE does not interact with the NP in any form. In case of intermediate pH regime (middle panels), it shows that the PE is highly localized at the surface of the NP. The peak for intermediate pH regime decreases with the increase in the NP separation. In NP separation r =41 Å, 62 Å, 88 Å the peak is 57, 39, 34 respectively. Similar behavior is seen in the high pH regime. The PE are localized at the NP surface and the peak value decreases as the NP separation increases.

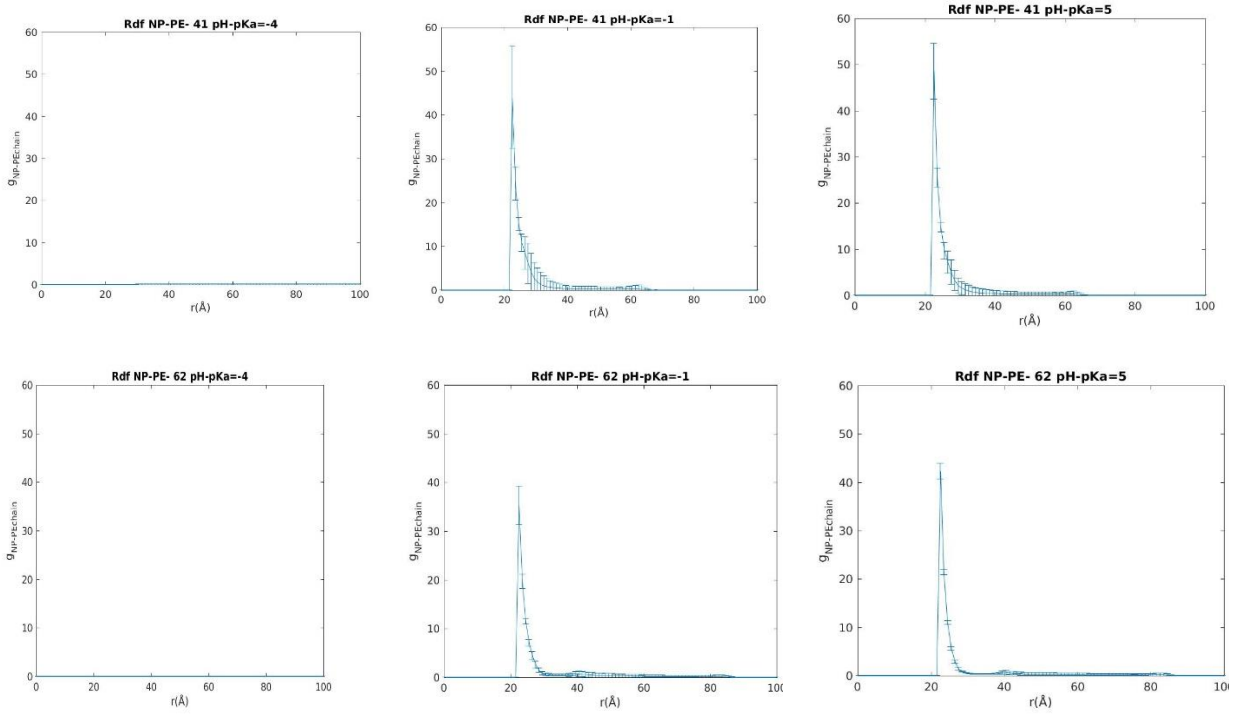

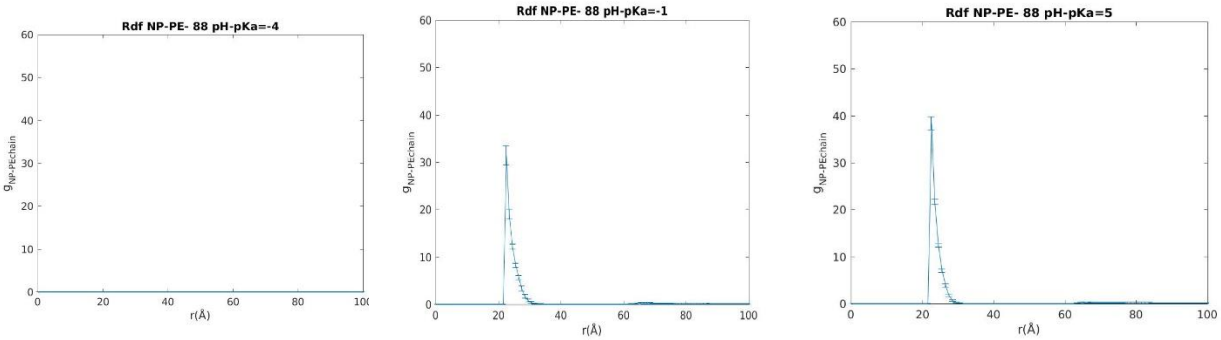

Figure 3-22 RDF of NP-counterion at different NP separation and different pH-pK_a

3.4.3. Bridge Formation

When the PE is adsorbed to both NPs simultaneously, we can consider that it forms bridge between the NPs.

At any given instant, the PE can interact with none of the NPs, 1 NP or with both NPs. The conformation of the PE, charge distribution along the PE chain, mean force between the NPs can change drastically in these three conditions.

Figure (3-23) shows the fraction of configurations where the PE is adsorbed to both NP i.e. forming a bridge as a function of NP separation. Figure () shows the fraction of configuration where the PE is adsorbed to 1 NP only.

Figure (3-23) shows that the for small separation r < 45 Å, the PE forms bridge in all pH regimes except for pH-pK0= -4. This happens because all the charged particles tend to concentrate in the space between the NPs. PE chain is long which takes up all the space between NP regardless the monomers are charged or not. The adsorption condition is thus satisfied to both the NPs. For the systems with pH-pK_0 = -3 , -2 a gradual decrease in bridge formation is observed with the increase

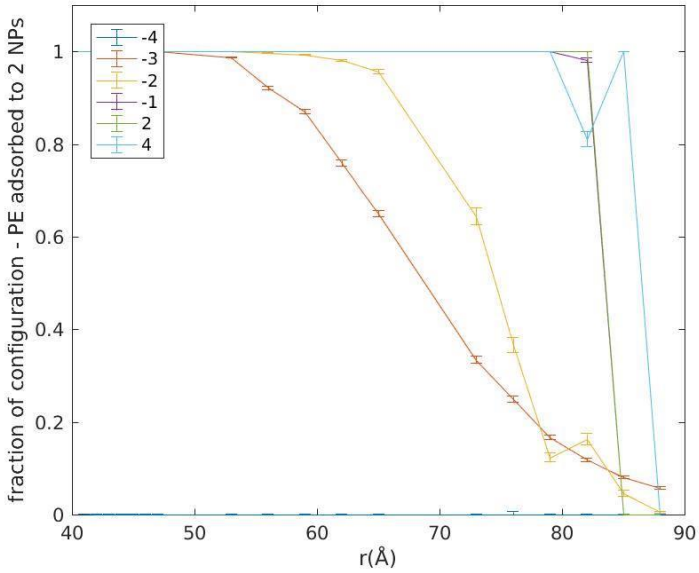

Figure 3-23 Fraction of configuration where the PE is adsorbed to both NPs as function of NP separation

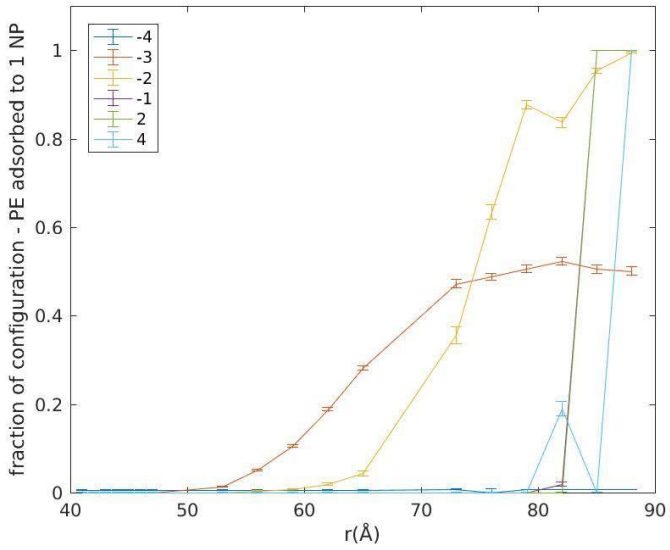

Figure 3-24 Fraction of configuration where the PE is adsorbed to both NPs as function of NP separation

in NP separation. For the systems above pH-$pK_a \geq$ -1, bridge is formed up to r = 85 Å and it breaks abruptly above that distance.

Figure (3-24) shows fraction of configuration where the PE is adsorbed to 1 NP only. For the system with pH-pK_a= -3 it increases gradually as the NP separation increases. It reaches the value about 0.5 and then remains constant with further separation. For pH-pK_a = -2 it increases gradually with the increase in separation. For the system pH-$Pk_a \geq$ -1, it increases to 1 abruptly at higher separation.

The fraction of configuration where PE is not adsorbed to any NP can be calculated from the two figures(3-23 3-24). Adding the fraction of configuration, the PE forms bridge and the fraction when it is adsorbed to 1 NP and subtracting from 1 gives the fraction of configuration the PE is not adsorbed to any NP. For the system with pH-pK_a = -3 at separation r= 73 Å, it is about 10%.

Radius of gyration

Figure (3-25) shows the radius of gyration of PE in presence of NP with varying NP separation at constant pH-pK_a.

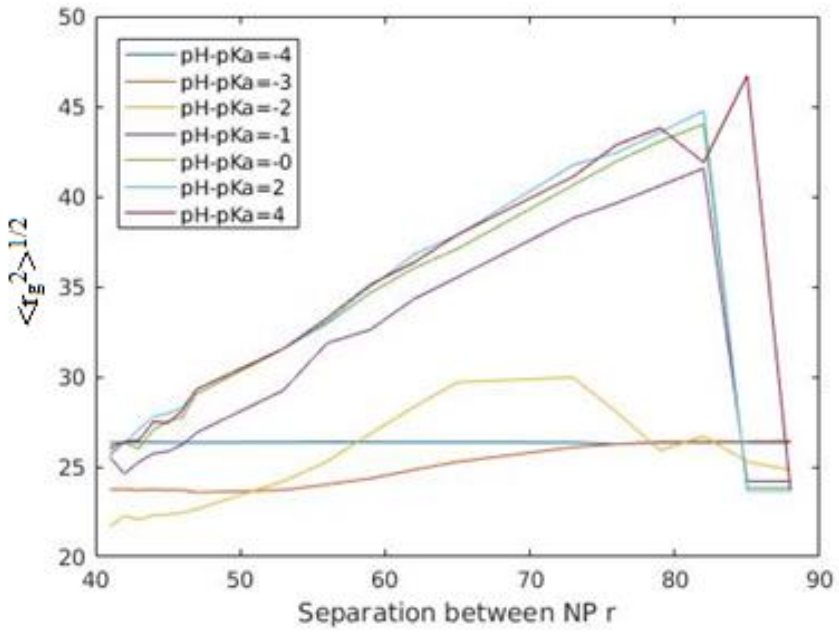

Figure 3-25 root mean square of radius of gyration at different pH-pKa as function of S_{NP}

In case of pH-pK_a= -4 the degree of ionization = 0 and hence has no effect of NP.

In case of pH-pK_a = -3 α varies from 0.3-0.06 with increasing NP separation. For smaller separation as the α is significant, the PE interacts with the NPs and the r_g is small. From figure(3-24), for larger separation, the PE is adsorbed to 1 NP 50% of the configurations, yet the r_g is comparable to that of uncharged PE it the system pH-pK_a. Radius of gyration increases as the charged monomers tend to repel each other or as it gets adsorbed to NPs and NP-NP separation increases. For this case NPs there are very few charged monomers in PE that are next to each other so the repulsive force is not strong to expand the PE chain. Also, as only few monomers are charged, PE is not well adsorbed at the NPs which doesn't decrease the radius of gyration. As the two effect doesn't contribute the r_g of the PE is comparable to the uncharged PE.

For pH-pK_a= -2 α varies from 0.6 - 0.4 as separation increases. For small separation, the r_g is considerably smaller than PE at α =0. This is due to the adsorption of PE in between the NPs. The r_g has a peak around the NP-NP separations r= 66 to r=73 which is due to the formation of bridge that elongates the chain. PE in system with NPs separated by r = 79 Å has an equal probability of forming bridge and adsorbing to 1 NP. r_g is the average of both the situations and hence for these separations r_g has decreased.

For pH-pKa= 0 and 2, r_g increases linearly up to r= 82 Å and abruptly decreases at r= 85 Å. This shows that the PE has formed bridge up to r =82 Å and then at r=85 Å PE completely interacts with 1 NP only.

It is important to note that the r_g for PE chain interacting with the NP is smaller than when the r_g of PE chain is calculate without NP. As PE gets adsorbed at NP, PE wraps around the NP decreasing the r_g. r_g can be plotted as the function of NP separation for sufficiently charged PE chains up to the separation where bridge forming is supported.

Comparison with strong PE

Strong PE is simulated for comparison at different NP separation with charge of monomers fixed at α corresponding to different pH-pK_a.

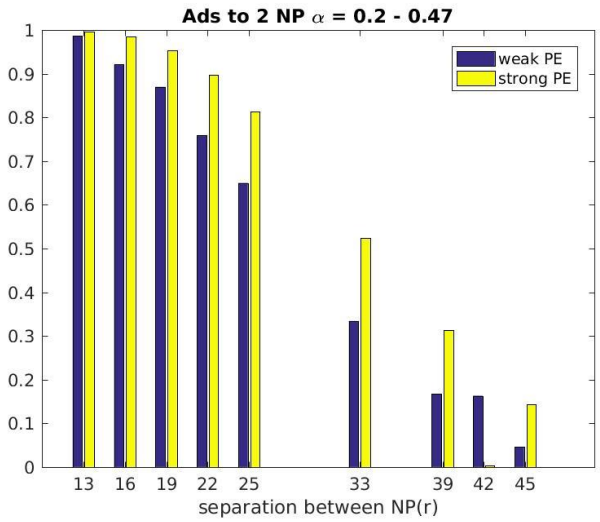

Figure 3-26 Comparative study of weak and strong PE forming bridge at different degree of ionization and different NP separation

Figure (3-26) shows the fraction of configuration of PEs, in the ensemble forming a bridge at different NP separation. The degree of ionization calculated from the weak PE is used as the charge of each monomers of PE and PE counterions of the strong PE.

In figure (3-26) it is clear that strong PE has a larger probability of forming bridge than weak PE of corresponding α. Weak PE prefers to wrap around 1 NP than bridge 2 NPs. The figure 3-23 shows that for small pH-pKa values PE is adsorbed to 1 NP than bridge 2 NP.

RDF of the system further elaborates the picture

Figure (3-27, 3-28, 3-29) shows the RDF of NP-PE of the weak PE at pH-pK_a = -3 at three differernt S_{NP}= 53 Å, 65 Å and 79 Å as well as the RDF of the strong PE with the corresponding α as the charge of the each monomer. The sharp peak of the weak PE curve at r = 22.5 Å shows that the PE is localised at the NP surface. The wider peak of the strong PE suggest that the strong PE is less localized but rather keeps a regular distnce from the NP surface. This comparison shows that the weak PE is adsorb to the NP than the strong PE.

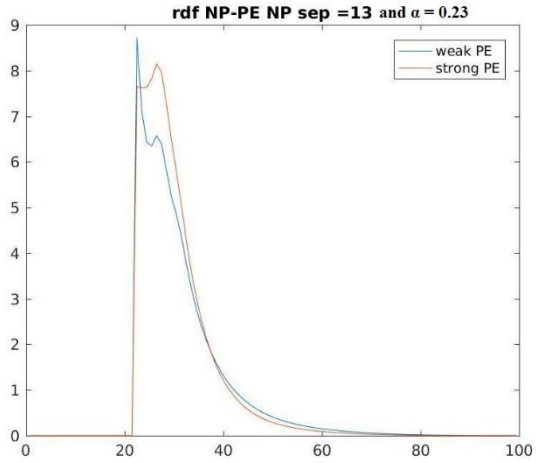

Figure 3-27Comparison between RDF of weak and strong PE S_{NP} = 43Å and α= 0.23

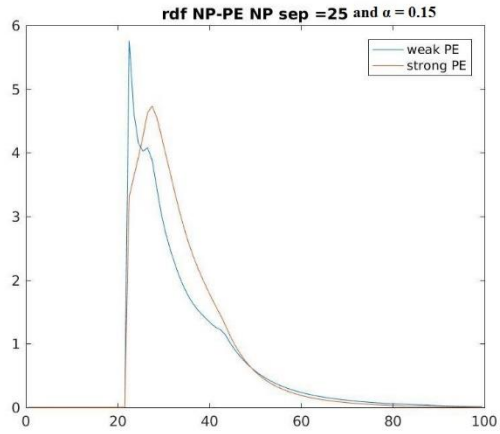

Figure 3-28 Comparison between RDF of weak and strong PE S_{NP} = 65Å and α= 0.15

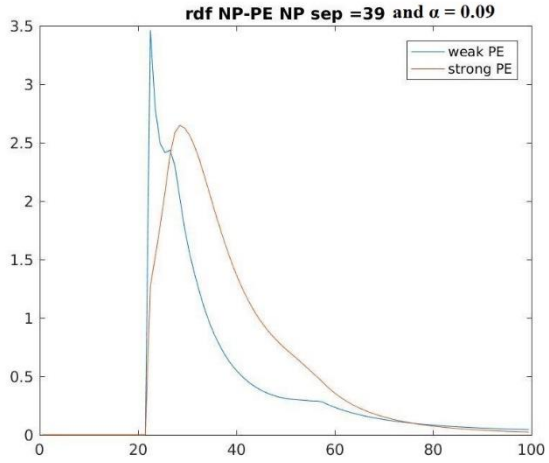

Figure 3-29 Comparison between RDF of weak and strong PE S_{NP} = 79Å and α= 0.09

In figure (3-31) the distribution of the particles along z-axis with weak PE at S_{NP}= 85 Å at pH-pK_a = -3 is shown and in figure (3-30) strong PE with charge of monomer equal to α of weak PE and same S_{NP} is given. In figure (3-31) the PE is found closer to the surface of the NP that faces the other NP. It signifies that the PE preferentially adsorbs to the gap between the NPs. In other hand,

the strong PE is more distributed at all distances in between NPs. It shows that the monomers of the PE are not necessarily adsorb at the surface but float in between the NPs.

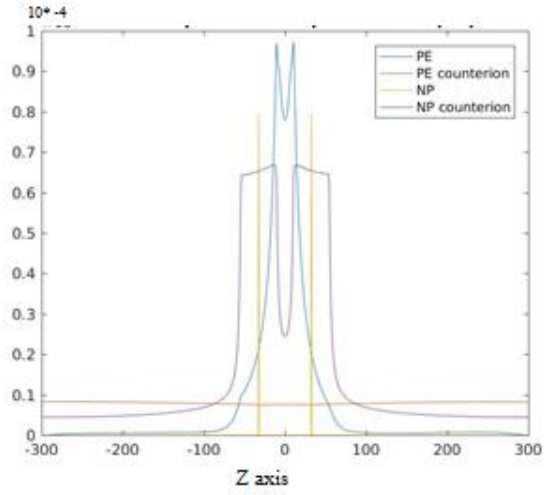

Figure 3-31 Particle distribution along z-axis for S_{NP} = 85 Å with weak PE at pH-pKa=-3

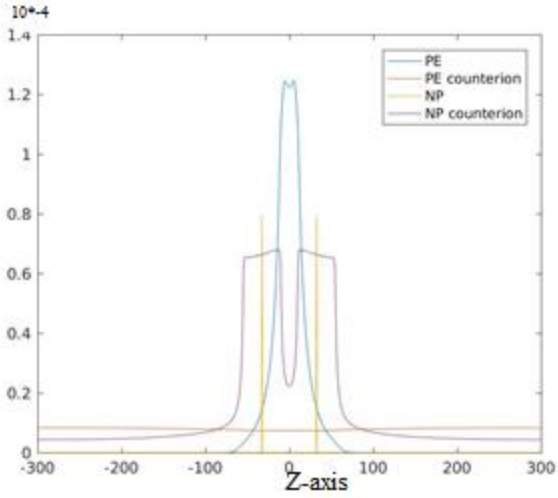

Figure 3-30 Particle distribution along z-axis for S_{NP} = 85 Å with strong PE at α = 0.15

The snapshot of the system with weak PE and strong PE is shown in the figure(3-29). The weak is adsorbed to the NP while the strong PE is floating in between the NPs.

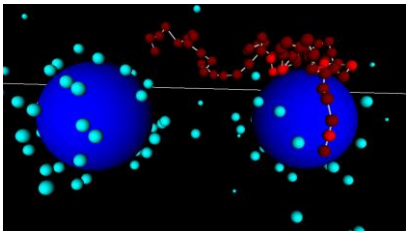

Figure 3-32 Snapshot of system of S_{NP} = 85Å and pH-pK_a = -3

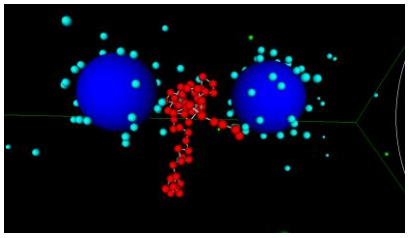

Figure 3-33 Snapshot of system of S_{NP} = 85Å at α = 0.15

3.5. Charge Distribution in monomers of PE

The charge distribution in monomers in presence of two NPs is compared with PEs alone. Only few selected systems are chosen.

Figure (3-34) and (3-35) shows the charge distribution along the PE chain at different S_{NP} and a comparison is done with the control system. Control system here is when only PE is simulated. In

case of PEs at pH-pKa = - 3 the degree of ionisation is nearly equal to 0 (check figure 3-10). To make a sensible comparison here the control system has the α = 0.13 computed at pH-pKa = -2.

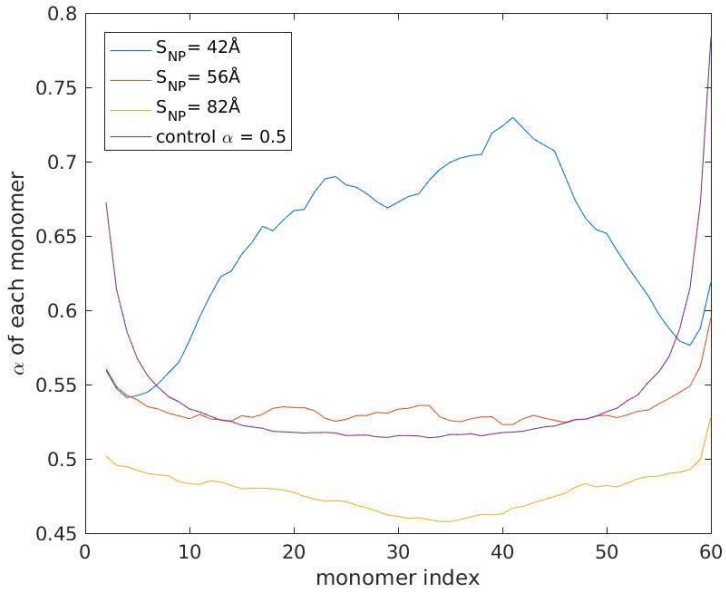

Figure 3-34 Average charge on each monomer of PE chain at different S_{NP} at pH-pK_a = -2.

From figure 3-34 it is seen that the end of the chain has a higher degree of ionization compare the monomers at the centre of the chain. When two NPs are present for the S_{NP}= 42 Å the monomers

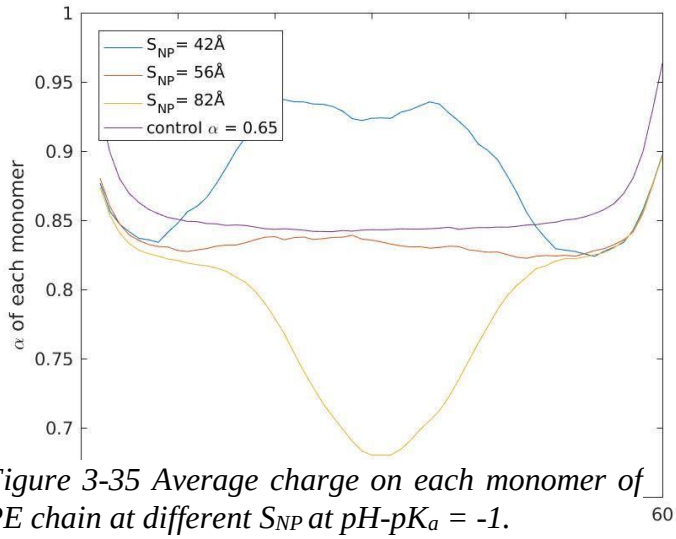

Figure 3-35 Average charge on each monomer of PE chain at different S_{NP} at pH-pK_a = -1.

at the centre of the chain has higher degree of ionisation compare to that of the end of the chain. From figure (3-23) for small separation PEs is adsorbed to both the NPs. This shows that the centre of PEs is more adsorbed to the NPs than the end of the chain. While we look at the curve for S_{NP} = 56 Å it also shows the similar case of the where the monomers the centre of the PE chain has more ionisation than the monomer at the end of the chain. In case of S_{NP}= 82 Å, there is no different to the monomer at the end or at the centre of the chain.

Figure 3-35 shows the charge distribution of PE chain at different S_{NP} at the pH-pK_a = -1. A corresponding control system is also plotted. For the small S_{NP} = 42 Å, the monomers at the centre of the PE chain has higher degree of ionisation compare to that of the end of the chain. This is similar to the figure 3-34. We can observe two maxima symmetric to the centre index. We can conclude that for small S_{NP} degree of ionisation does not affect the charge distribution of the monomers of PEs.

The curve for the S_{NP} = 82 Å is of interest. Here the monomers at the ends of PEs are charged significantly more than that of the monomers at the centre of the PEs. The monomers at the end of the chain therefore are adsorbed significantly more leading to formation of bridge at large S_{NP} = 82 Å. When the monomers are charged, it has higher attractive force with the NPs resulting in an adsorption. In case of weak PEs, the charge distribution within PEs are structured such a way that it enables adsorption with any NPs as possible.

3.6. Mean Force and Potential of Mean Force

The mean force between the NPs mediated by the counterion and the PE at different pH-pK_a and

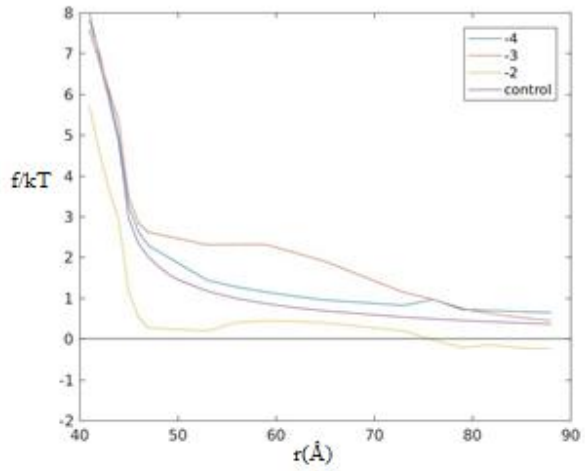

Figure 3-36 Mean force calculated for pH-pK_a = -4, -3, -3 and the control system as a function of S_{NP}.

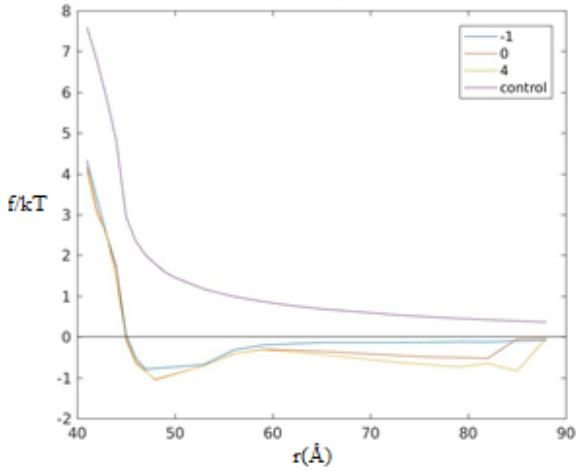

Figure 3-37 Mean force calculated for pH-pK_a = -1, 0, 4 and the control system as a function of S_{NP}.

S_{NP} is discussed.

Figure (3-36) shows the mean force curve for the pH-pK_a = -4 to -2. Figure (3-37) shows the mean force curve for the pH-pK_a = -1, 0, 4. Mean force for the control system is also shown. Control system has NPs and its counterions only.

In figure (3-37) the mean force for pH-pK_a= -4, -3 and control system is always repulsive. At S_{NP} = 41 Å which is just above contact, the force is maximum. In the range, S_{NP} = 41 Å to S_{NP} = 47 Å mean force at pH-pKa -4, -3, and control system are the same.

Mean force curve for pH-pKa = -3 does not decay as it does for the other curves for the S_{NP}= 53 Å to S_{NP} = 65 Å, there is an increment in f(53) to f(65). For S_{NP} > 65 Å mean force decreases but does not decay to zero.

For the system pH-pKa = -2 the curve sharply decreases from S_{NP}= 41 Å to S_{NP}= 47 Å and then remains fairly constant near to value zero. At NP contact distance f(41) = 8 kT for pH = -4,-3 and control system. For the system at pH = -2, mean force at contact is f(41) ≅ 6 kT.

Figure (3-37) shows the mean force curve for the systems pH-pK_a = -1, 0 and 4. An attractive well is observed at S_{NP}= 48 Å for all the system with pH-pKa ≥ -1. The depth of the well is -1 kT for all the systems. For the S_{NP} > 48 Å the well decays. In case of pH-pK_a = -1 it decays to zero, but in the other cases pH-pK_a ≥ 0 it seems to have a second minimum.

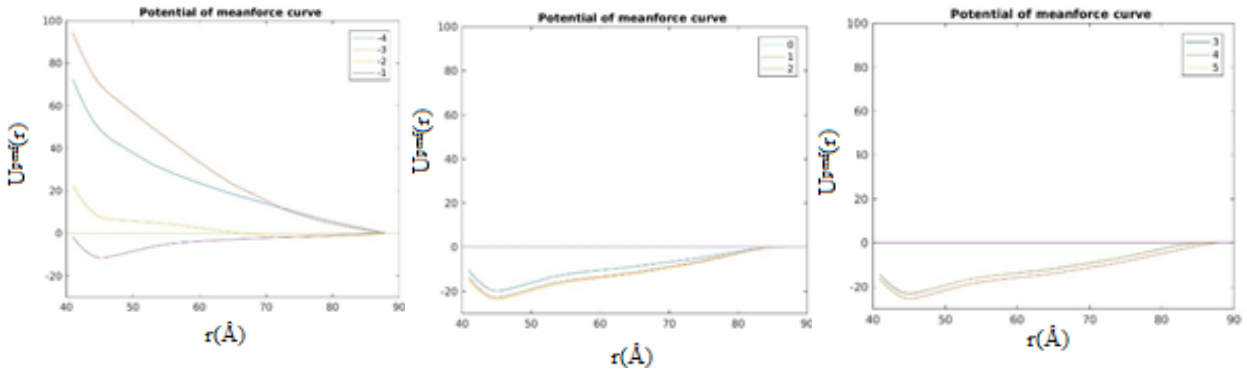

Figure 3-38 Potential of mean force for different pH-pKa as a function of S_{NP}.

In figures (3-38) potential of mean force is given. As the mean force have not decayed to zero the conventional U^{pmf} = 0 at infinite separation cannot be employed. Here, U^{pmf} (r = 88) = 0 has been assigned. At r ≥ 88 Å bridge formation is not possible for all pH-pKa systems. The interaction between the two NPs negligible. Therefore, U^{pmf} (r = 88) = 0 assigned.

At pH-pK_a = -4 and -3 very strong repulsion at the two colloids appears at short separation. The repulsion for pH-pK_a = -3 is more than that of -4. For pH-pKa = -2 the repulsion is reduced to 20 kT for the short separation. For the system with pH-pK_a > -2 a minimum is formed at S_{NP} = 48 Å. The depth of the minimum varies slightly with change in the increment of pH-pK_a becoming deeper with increasing ionization, as would be expected.

The mean force is calculated by from 4 components as explained in the equation 16. Figure 3-39 and 3-40 shows the component of mean force for two representative systems at pH-pKa = -3 and 4 respectively. $F_{ideal}(r)$ is always repulsive. It decays as S_{NP} increases. Ideal force is measured as

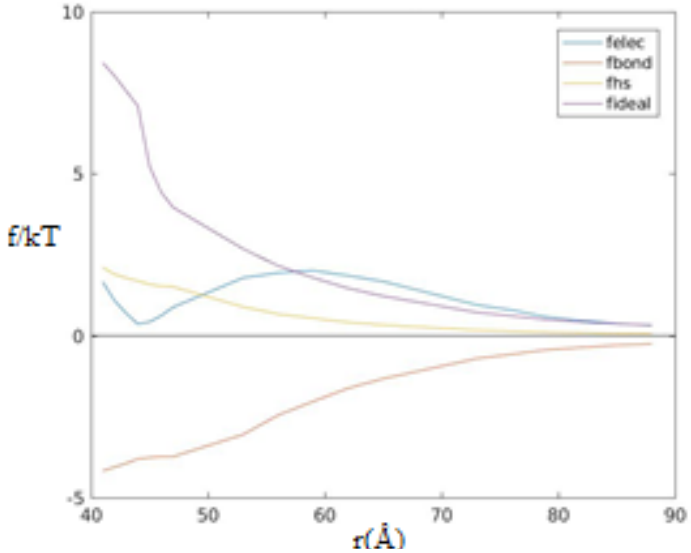

Figure 3-40 Components of mean force calculated at pH-pK_a = -3

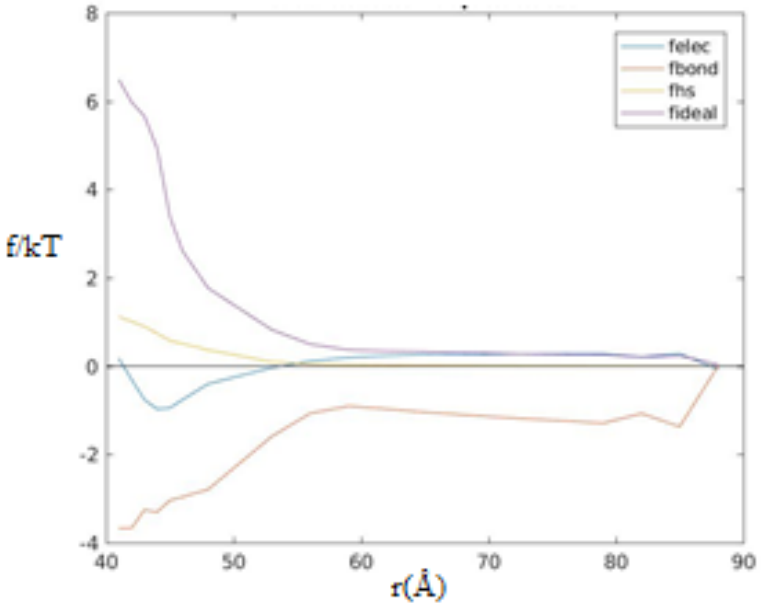

Figure 3-39 Components of mean force calculated at pH-pK_a = -3

the difference in the number density at the z = 0 plane and z = $L_{cyl}/2$ plane. As the NP separation increases the particles move away from the center z = 0 plane and so the f_{ideal} force decreases.

The hard sphere contribution, $f_{hs}(r)$ appears at the short separation and decays to zero smoothly. $F_{elec}(r)$ is the electrostatic force. For the short separation, it decreases as S_{NP} increases readily to a minimum S_{NP} = 45 Å. This is due to the counterions correlation. F_{elec} increases further becoming more repulsive at around r = 65 Å. There after f_{elec} decreases to zero at layer larger separations. $F_{bond}(r)$ is the principle contributor to attractive force. It is maximum at the short separation and decays to zero as the separation increases.

Figure (3-40) shows the mean force components for the pH-pK_a = 4. In this system, the PE is highly charged and a bridge is formed between NPs for all system except at S_{NP} = 88 Å. F_{ideal} (r) is always repulsive in case too. The magnitude of $f_{ideal}(r)$ is nearly 1kT less than that of previous system. $F_{ideal}(r)$ also decays more rapidly compare to the previous system and approaches to zero. Figure 3-31 shows that in system with two NPs and charged PE, PE is found in the space between the NPs. The presence of the PE displaces the counterion from the space between the NP to the other face. Decrease in density of the particles at z = 0 plane decreases f_{ideal} as it is calculated from the difference in the number density at z = 0 plane and at z = $\pm$ $L_{cyl}/2$ plane. As the distance increases density of NP counterions further decreases leading to the decrease in f_{ideal} force.

Hard sphere force $f_{hs}(r)$ appears at the short separation and decays immediately. The electrostatic contributor $f_{elec}(r)$ is attractive contrary to the previous system. The minimum appears at S_{NP} = 46Å. This component is attractive because of the correlation of the monomers. The monomers adsorbed to a NP attracts NP in other side and the mean force in appears to be attractive.

The largest contributor to the attractive mean force is the bond term. It has the maximum value at the short separation and it decays as separation increases. From the S_{NP} = 56 Å to S_{NP} = 85 Å it remains constant and abruptly decays to zero at r=88 Å. The bond force is measured across the plane z = 0 (equation 20). If the bridge is present there will be bonds across the z = 0 plane contributing to the bond force.

3.6.1. Comparison with free NPs

So far in all the system the NPs were fixed at a certain separation, centered at z=0.

The mean force and the potential of the mean force calculated by this method showed a potential well at NP separation r = 47 Å. We have performed more calculations where the NPs were free to move along the z-axis. The cluster move was used. In this type of move when the NP is moved the counterions and the PE monomers in a certain radius around it are moved together. This increses the number of Monte Carlo accepted moves and imporves the sampling of the system.

RDF between NP-NP are given in the figures below.

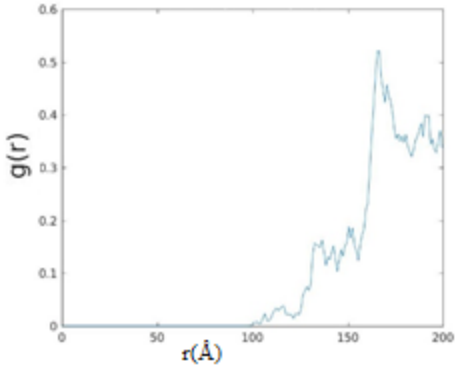

Figure 3-41 RDF between NP-NP with moving NPs at pH-pKa = -2

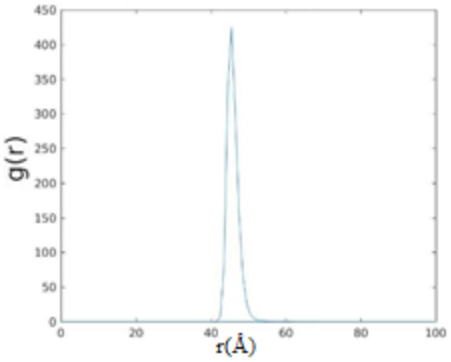

Figure 3-42 RDF between NP-NP with moving NPs at pH-pKa > -1

In the case of pH-pK_a = -2 the repulsive force is prevalent. NPs are not found in the proximity of each other. In case of pH-pK_a≥ -1 the rdf of NP-NP is found to peak at r = 46 Å which agrees with the mean force and potential of mean force calculated.

4. Conclusion

Monte Carlo method has been used to study the interaction between a weak PE chain with two oppositely charged NPs. A primitive model of the electrolytes where the particles are represented as hard-spheres differing in size and charge has been used. The NP-NP separation (S_{NP}) and pH-pKa of the solution is varied.

The investigation commenced by study of 1 NP system and distribution of its counterion, comparing that with 2 NPs system with its counterion. We have found that the counterions in both the systems are highly adsorbed to the NP surface. In case of 1NP system, counterions are symmetrically distributed around the NP. In case of 2 NPs system the space between the NPs has more concentration of counterions than the other face of NPs. The RDF of NP-counterions in 1NP

system is 3 times higher than the system with 2 NPs. As the NP surface area of 2 NP system is higher than the 1NP system, the density of localized counterion decreases for 2 NP system.

Next in line is to study the PE chain conformation without the presence of NPs. Titration curve shows that $\alpha = 0.5$ is achieved for pH-pKa = 2. RDF of weak PE chain and its counterion is calculated and is also compared with the corresponding strong PEs. The interaction between the weak PE chain and its counterion is found to be stronger compare to that of strong PEs. Counterions in weak PEs tends to concentrate at the PE monomer surface as degree of ionization $\alpha > 0.5$. In case strong PE such behavior is seen only after $\alpha > 0.7$. Electrostatic force between the weak PEs monomers and counterion is much stronger than with strong PEs as charge in the weak PEs are unity and that of strong PE is fractional.

Radius of gyration of weak and strong PEs in absence of NPs is studied. It is found that the r_g is relatively larger for the strong PE chain than weak PE chain. Weak PE chain has higher counterion condensation which effectively neutralizes the repulsive force among the neighbor charged monomer reducing the expansion of the chain.

Presence of NPs extremely influences the titration. We found that the inflection point is shifted to much lower pH-pKa compare to the free PE chain. S_{NP} also influences the tritation. Short separation leads to higher α at lower pH-pKa.

RDF of the NP with its counterions and PE study shows that the counterions are localized at the NP surface. Charged PEs chain are also localized to the NP surface but the uncharged NP chaina does not interact with the NPs.

We investigated the formation of bridge between NPs and interacting to only 1 NP. We observed that at pH-pKa = -4 PEs chain does not form interact with NP at all. At pH-pKa = -3 and -2 PE chain bridge completely at small S_{NP} and gradually decreases with increasing S_{NP}.

Radius of gyration of PEs chain is govern its interaction with NPs. We observed that at pH-pKa ≥ -1, r_g gradually increases as S_{NP} increases and abruptly breaks at S_{NP} = 85 Å. This is because the PE chain forms bridge between NPs up to S_{NP} = 82 Å and bridge breaks above S_{NP} = 85.

For $0.2 \leq \alpha \leq 0.47$ strong PE chain form bridge more frequently than the weak PE chain. Comparing the RDF of NP and PE chain reveals that the weak PE chain is localized at the NP surface and the strong PE is more distributed to the space between the NPs. We can conclude that weak PEs have stronger interaction with NPs than the strong PEs.

Interaction with NPs changes the charge distribution among the monomers in the PE chain. In case of the free PE chain, monomers at the end of the chain are more charged. In case of low pH-pKa solution the monomers at the centre of the chain is more charged compared to the monomers at the end of the chain. At the intermediate pH-pKa = -1 S_{NP} = 82 Å monomers at the end of the chain has α around 20 % higher than the monomers at the centre. This shows that the monmers adsorbed to NPs have more charged than other monomers.

Mean force between the NPs mediated by the NPs counterion, and PEs are calculated. In the system with only NP the mean force is always repulsive. In presence of the PEs at pH-pKa = -4 to pH-pKa = -2, the force is still repulsive. At pH-pKa > -2, attractive well is induced at short separation. The component wise study shows that f_{ideal} and f_{hs} components contribute to the repulsive force, while the f_{elec} and f_{bond} are the attractive force. F_{elec} arises from the adsorbed PEs chain correlation. Potential of mean force also shows a potential well for small separation. When the NPs are allowed to move along the z-axis, at pH-pKa $\geq$ -1, RDF of NP-NP peaks at 47 Å, which corresponds to the calculated potential of mean force.

As seen in the previous studies many factors affect the interaction of PEs with NPs like chain length, surface charge, radius of the particles, PE charge to NP charge ratio, density of the particles. Further study with different variation is required to completely understand the interaction between the PEs and NPs.

5. References

1. Berret J-F, Schonbeck N, Gazeau F, El Kharrat D, Sandre O, Vacher A, et al. Controlled Clustering of Superparamagnetic Nanoparticles Using Block Copolymers: Design of New Contrast Agents for Magnetic Resonance Imaging. Journal of the American Chemical Society. 2006;128(5):1755-61.

2. Schwoyer WLK. Polyelectrolytes for water and wastewater treatment1981.

3. Per L. Mean force between like-charged macroions at high electrostatic coupling. Journal of Physics: Condensed Matter. 2002;14(49):13449.

4. Linse P. Simulation of Charged Colloids in Solution. In: Holm C, Kremer K, editors. Advanced Computer Simulation Approaches for Soft Matter Sciences II. Berlin, Heidelberg: Springer Berlin Heidelberg; 2005. p. 111-62.

5. Salerno KM, Frischknecht AL, Stevens MJ. Charged Nanoparticle Attraction in Multivalent Salt Solution: A Classical-Fluids Density Functional Theory and Molecular Dynamics Study. The Journal of Physical Chemistry B. 2016;120(26):5927-37.

6. Ulrich S, Seijo M, Laguecir A, Stoll S. Nanoparticle Adsorption on a Weak Polyelectrolyte. Stiffness, pH, Charge Mobility, and Ionic Concentration Effects Investigated by Monte Carlo Simulations. The Journal of Physical Chemistry B. 2006;110(42):20954-64.

7. Ulrich S, Seijo M, Stoll S. The many facets of polyelectrolytes and oppositely charged macroions complex formation. Curr Opin Colloid In. 2006;11(5):268-72.

8. Carnal F, Stoll S. Adsorption of Weak Polyelectrolytes on Charged Nanoparticles. Impact of Salt Valency, pH, and Nanoparticle Charge Density. Monte Carlo Simulations. The Journal of Physical Chemistry B. 2011;115(42):12007-18.

9. Ulrich S, Seijo M, Carnal F, Stoll S. Formation of Complexes between Nanoparticles and Weak Polyampholyte Chains. Monte Carlo Simulations. Macromolecules. 2011;44(6):1661-70.

10. Dias RS, Pais AACC, Miguel MG, Lindman B. Modeling of DNA compaction by polycations. J Chem Phys. 2003;119(15):8150-7.

11. Ullner M, Jonsson B, Widmark PO. Conformational Properties and Apparent Dissociation-Constants of Titrating Polyelectrolytes - Monte-Carlo Simulation and Scaling Arguments. J Chem Phys. 1994;100(4):3365-6.

12. Wallin T, Linse P. Monte Carlo simulations of polyelectrolytes at charged micelles .1. Effects of chain flexibility. Langmuir. 1996;12(2):305-14.

13. Carnal F, Clavier A, Stoll S. Polypeptide-Nanoparticle Interactions and Corona Formation Investigated by Monte Carlo Simulations. Polymers. 2016;8(6):203.

14. Carlsson F, Linse P, Malmsten M. Monte Carlo Simulations of Polyelectrolyte−Protein Complexation. The Journal of Physical Chemistry B. 2001;105(38):9040-9.

15. Trizac E, Samaj L. Like-charge colloidal attraction: A simple argument. P Int Sch Phys. 2013;184:61-73.

16. Ulrich S, Laguecir A, Stoll S. Complexation of a Weak Polyelectrolyte with a Charged Nanoparticle. Solution Properties and Polyelectrolyte Stiffness Influences. Macromolecules. 2005;38(21):8939-49.

17. Carnal F, Ulrich S, Stoll S. Influence of Explicit Ions on Titration Curves and Conformations of Flexible Polyelectrolytes: A Monte Carlo Study. Macromolecules. 2010;43(5):2544-53.

18. Skepo M, Linse P. Complexation, phase separation, and redissolution in polyelectrolyte-macroion solutions. Macromolecules. 2003;36(2):508-19.

19. Jonsson M, Linse P. Polyelectrolyte-macroion complexation. I. Effect of linear charge density, chain length, and macroion charge. J Chem Phys. 2001;115(7):3406-18.

20. Reed CE, Reed WF. Monte-Carlo Study of Titration of Linear Polyelectrolytes. J Chem Phys. 1992;96(2):1609-20.

21. Katchalsky A, Shavit N, Eisenberg H. Dissociation of Weak Polymeric Acids and Bases. J Polym Sci. 1954;13(68):69-84.

22. Ullner M, Jonsson B. A Monte Carlo study of titrating polyelectrolytes in the presence of salt. Macromolecules. 1996;29(20):6645-55.

23. Ullner M, Jonsson B, Soderberg B, Peterson C. A Monte Carlo study of titrating polyelectrolytes. J Chem Phys. 1996;104(8):3048-57.

24. Wang SQ, Granick S, Zhao J. Charge on a weak polyelectrolyte. J Chem Phys. 2008;129(24).

25. Rescic J, Linse P. MOLSIM: A modular molecular simulation software. Journal of Computational Chemistry. 2015;36(16):1259-74.

26. Linse P. Interaction between colloids with grafted diblock polyampholytes. J Chem Phys. 2007;126(11).